

## Effect of impurities on the optical properties of KTP single crystals grown from flux

H Zaliani<sup>1</sup>, M Ja'far Tafreshi<sup>1</sup>, and D Souri<sup>2</sup>

1. Department of Physics, Semnan University, Semnan, Iran

2. Department of Physics, Faculty of Science, Malayer University, Malayer, Iran

(Received 11 May 2015 ; in final form 12 June 2016)

### Abstract

In the present work,  $\text{KTiOPO}_4$  (KTP) crystals have been grown by spontaneous nucleation technique in flux medium using  $\text{K}_6\text{P}_4\text{O}_{13}$  flux. Cooling rates of  $0.4\text{--}1\text{ }^\circ\text{C/h}$  were applied in the spontaneous nucleation process. The presence and amount of impurities has been determined by using X-Ray Fluorescence (XRF). The optical transmission spectra of impure KTP crystals in the UV–Visible region are discussed. The transmission cut-off is clearly shown at the optical absorption edge, as well as the rapidly reduced absorption with increasing wavelength. It is shown that the presence of impurity shifts the absorption edge of KTP towards lower energy region. The wavelength dependence of absorption coefficient is determined in the UV–visible range, and the characteristics of the optical absorption edge are discussed. Results reveal that the absorption edge and the type of optical charge carrier transition can be attributed to indirect transition for these crystals. It is shown that presence of impurity decreases the indirect band gap ( $E_g$ ) of KTP crystals, causing the indirect transition absorption edge to move towards lower energy. Also, structural characterization was carried out employing XRD and IR analysis, confirming the growth of KTP crystal.

**Keywords:** spontaneous nucleation method, KTP crystals, energy gap, transmission spectrum, flux method

### 1. Introduction

Excellent characteristics like high thermal stability, good mechanical properties, transparency over a large wavelength range, large nonlinear-optical coefficients, high damage threshold, and broad angular acceptance have made potassium titanyl phosphate ( $\text{KTiOPO}_4$ ; KTP) as an excellent crystal for second-harmonic conversion of Nd:YAG laser radiation [1-2]. The presence of impurities in  $\text{KTiOPO}_4$  (KTP) single crystals can have severe consequences in the performance of devices made from these crystals, for example the optical absorption in the green-wavelength regime leads to a detrimental effect on their Second-Harmonic Generator (SHG) performance [3], so the characterization of the spectroscopic properties of impurities in bulk crystals is important.

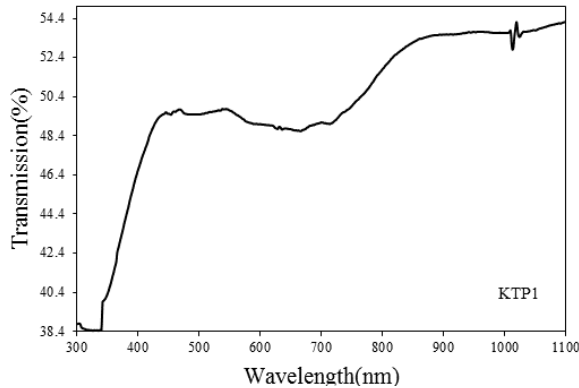
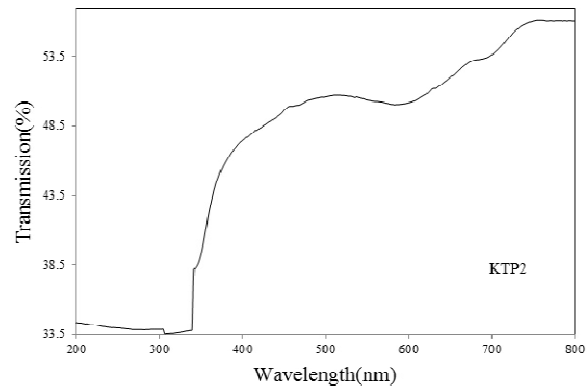
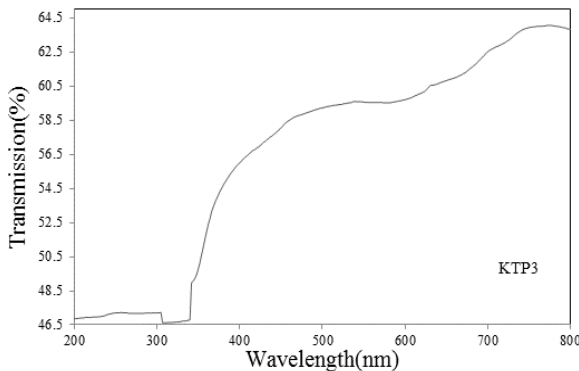
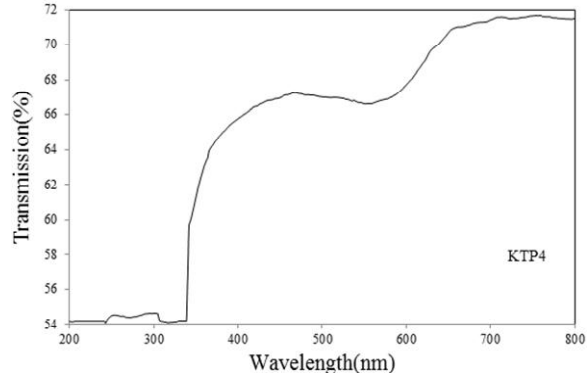
Because of KTP decomposition upon melting at  $1172\text{ }^\circ\text{C}$ , its growth in the single-crystal is mainly done by two main growth methods, namely, the hydrothermal method and the flux method [4-10]. The flux method seems to be superior to the hydrothermal method in almost every respect such as quality, size, growth velocity and costs [11-12]. In addition, although this method has the disadvantages of incorporation

of OH, it is currently the most popular method for obtaining large KTP single crystals. Among the choices from phosphates, tungstates, molybdates, etc. as solvent, polyphosphate  $\text{K}_6\text{P}_4\text{O}_{13}$  has been identified as the most suitable for the crystal growth of KTP crystals because it does not contain any ion different from those in KTP [9]. But even after avoiding the possibility of impurity incorporation in the crystal by choosing this self-flux, one is left with at least two more possibilities of contamination. One, of course, is from the starting chemicals, and the other one is through impurities from the crucible [3].

There are many reports on the growth and quality of KTP crystals [13-21]; reporting that KTP crystals of adequate quality for the applications mentioned have been grown from a potassium-phosphate flux system (especially  $\text{K}_6\text{P}_4\text{O}_{13}$ ) [13]. Bolt et al. [13] and Halfpenny et al. [14] showed low dislocation density in flux grown KTP, which was investigated by means of X-ray topography using characteristic X-ray radiation and synchrotron white radiation, respectively. Yokotani et al., [15] showed that optically uniform devices could be obtained when a single growth sector chosen by means

**Table 1.** The properties of growth for four samples.

Samples	Growth technique	Cooling rate (°C/h)	Growth time (h)	Transmission (%)
KTP1	Spontaneous Nucleation (SN)	1	170	53.67
KTP2	Spontaneous Nucleation (SN)	0.8	250	56.055
KTP3	Spontaneous Nucleation (SN)	0.4	307.5	64.02
KTP4	Nucleation on Rod (NR)	0.7	182	71.631

**Figure 1.** The optical transmission spectrum of KTP crystal grown from  $K_6$  flux by spontaneous nucleation with cooling rate of 1 °C/h; KTP1.**Figure 2.** The optical transmission spectrum of KTP crystal grown from  $K_6$  flux by spontaneous nucleation with cooling rate of 0.8 °C/h; KTP2.**Figure 3.** The optical transmission spectrum of KTP crystal grown from  $K_6$  flux by spontaneous nucleation with cooling rate of 0.4 °C/h; KTP3.**Figure 4.** The optical transmission spectrum of KTP crystal grown from  $K_6$  flux by nucleation on rod with cooling rate of 0.7 °C/h; KTP4.

of laser interferometry was used. However, Sasaki et al. [16] found that each sector had a distribution of refractive indices and had problems obtaining large areas for nonlinear devices.

In the present study, single crystals of  $KTiOPO_4$  were grown using the slow cooling flux method in the three and single-zone furnace system. It was observed that transmission window of KTP crystals are very wide ranging. We have three purposes in the present work; the first is to study the optical spectrums and determining peaks, the second is to reveal impurities by XRF analysis and the third is to consider the effect of these peaks as well as impurities on band gap of crystals. There have been reports that some kinds of impurities, such as Si, Al, Ca, Pb, Fe and Nb are responsible for absorbance in KTP [17]. In our grown KTP crystals, the XRF analysis revealed these impurities at the threshold detection level. However, the Pt and Rh impurities were detected and measured to be 0.06%.

## 2. Crystal growth experimental details

KTP single crystals were grown by the flux growth technique without a seed crystal. The prepared raw material and flux

( $K_6$  flux) were mixed in a definite ratio and a suitable amount of the mixture was put into an open platinum crucible consisting of 5-10% Rh with 50 mm in diameter and 50 mm in height. The purities of the initial components were in the 99.5%- 99.95% range. The assembly was heated to 1050 °C to melt the mixture, and then crystal growth was carried out. The growth of the KTP crystals was accomplished by slow cooling in an appropriate temperature gradient [22]. The properties of growth (for KTP1, KTP2, KTP3 and KTP4 samples) are presented in table 1.

## 3. Characterization

### 3.1. Optical spectroscopy

The grown crystals were cut and were polished into small specimens of thickness about 1mm and subjected to optical transmission measurements in the spectral region of 300–800 nm using a Shimadzu (UV-PC-3101) UV-VIS spectrophotometer. A large number of KTP crystals were examined during this study. The transmission spectra for different samples in different status are shown in figures 1-4. In these figures, we show the optical transmission spectra of KTP crystals grown

**Table 2.** The different impurities percent for KTP samples.

Sample	KTP1	KTP2	KTP3	KTP4
Element's oxide	%			
Nb <sub>2</sub> O <sub>5</sub>	0.010	0.011	0.014	0.010
Fe <sub>2</sub> O <sub>3</sub>	0.034	0.026	0.070	0.029
CaO/PbO	0.046% (CaO)	0.049 (CaO)	0.11 (CaO)	0.095 (PbO)
Al <sub>2</sub> O <sub>3</sub>	0.20	0.19	0.38	0.12
SiO <sub>2</sub>	0.654	0.597	1.09	0.40
K <sub>2</sub> O	22.45	22.31	25.66	22.01
P <sub>2</sub> O <sub>5</sub>	28.6	29.9	32.1	28.1
TiO <sub>2</sub>	33.46	34.45	40.16	33.89

by spontaneous nucleation and nucleation on rod.

### 3.2. XRF analysis

X-Ray Fluorescence (XRF) studies were carried out using Bruker diffractometer XRF "Germany" to check the presence of impurities in the grown crystals [3]. The impurities percent for different samples are shown in table 2.

The presence of some expected impurities was confirmed; Rh was diffused from the crucible walls. Other unexpected impurities were also found, the most significant one being Si and then Al. Small concentrations of Fe, Ca, Pb and Nb were also determined. Also, XRF analysis carried out on the Pt crucible used for the growth of colored crystals of KTP confirmed the presence of Rh impurity in the crucible. Thus, the crucible used for growing this particular crystal was identified as the source of Rh impurity in the crystal. The Pt and Rh impurities were detected and measured to be 0.06%.

### 3.3. XRD analysis

The structural characterization of the KTP samples was carried out by X-Ray Diffractometry (XRD) using a Bruker diffractometer (AXS D8 Advance, CuK $\alpha$ : 1.5406 Å). XRD pattern of typical sample KTP3 is shown in figure 5 (a and b), to confirm the growth of KTP crystal and the existence of Rh impurity, respectively.

### 3.4. IR analysis

The Fourier Transform Infrared absorption spectrum of the produced KTP crystal was recorded at room temperature on a Shimadzu 8400S system over a spectral range of 400-4000 cm<sup>-1</sup>, to determine the structural units and therefore to confirm the growth of KTP crystal. Typical plot of IR spectra is presented in figure 6.

## 4. Band gap and absorption cut off

Incorporation of impurity ion considerably decreases the overall transmittance of KTP and it can be explained by the increases of absorption coefficient ( $\alpha$ ), which can be evaluated by Mclean formula [13]. Miyamoto et al. [17] reported that the incorporation of Pt impurities from the crucible increases the optical absorption coefficient of KTP [23]. In the low energy area,  $\alpha$  is proportional to  $\exp(h\nu)$ , while in the high energy field,  $\alpha$  obeys the following relationship:

$$(\alpha(\nu)h\nu) \propto (h\nu - E_{\text{gap}})^m, \quad (1)$$

where,  $E_{\text{gap}}$  and  $h\nu$  are the optical gap and incident

photon energy, respectively; and  $\alpha(\nu)$  is the absorption coefficient defined by the Beer-Lambert's law as:

$$\alpha(\nu) = (2.303/d)A, \quad (2)$$

where,  $d$  and  $A$  are the sample thickness and sample absorbance, correspondingly [19]. Also,  $m$  is the index which determines the type of optical charge carrier transmission.

In order to obtain  $E_{\text{gap}}$  (upon Eq.1), it was necessary to measure the absorption coefficient ( $\alpha$ ) which was carried out by measuring the film thickness and film absorbance. In this work, we used the absorption spectrum fitting method (ASF) [24] to obtain the band gap avoiding the film thickness measurement which commonly could not be measured precisely.

Thus, applying the ASF method, from eq. (1) and eq. (2) we have [24]:

$$\left(\frac{A}{\lambda}\right)^{1/m} \propto \left(\frac{1}{\lambda} - \frac{1}{\lambda_g}\right), \quad (3)$$

where,  $E_g$  is the optical energy gap,  $m = 1/2$  is applied for direct transition and  $m = 2$  is applied for indirect transition. KTP is an indirect gap material [5]; thus, the  $m$ -value for KTP is 2, which this optimized value was obtained by examination of the different values of  $m$ , by using the least square technique.

Thus, the value of band gap, in eV, can be calculated from the parameter  $\lambda_g$  using  $E_{\text{gap}} = 1239.83/\lambda_g$ . In other word, the value of  $\lambda_g$  can be calculated by extrapolating the linear region of  $(A/\lambda)^{1/2}$  vs.  $(1/\lambda)$  curve at  $(A/\lambda)^{1/2} = 0$ . The variation of  $(A/\lambda)^{1/2}$  vs.  $(1/\lambda)$  was plotted for the present samples, as shown in figures 7-10; the data of optical band gap for different samples have been listed in table 3.

## 5. Discussion

Some crystals grown in platinum crucible containing Rh as impurity were reddish-orange in color. Because of platinum being soft, sometimes manufacturers add rhodium deliberately to increase the strength of the platinum crucible. The platinum group metals require rather complex aqueous chemical processing for their isolation [25]. This increases the probability of occurrence of Rh in Pt crucible. Because the growth period of KTP crystal is high, Rh ions get into the molten charge through diffusion. Repeated growth runs performed from the old charge and from the same

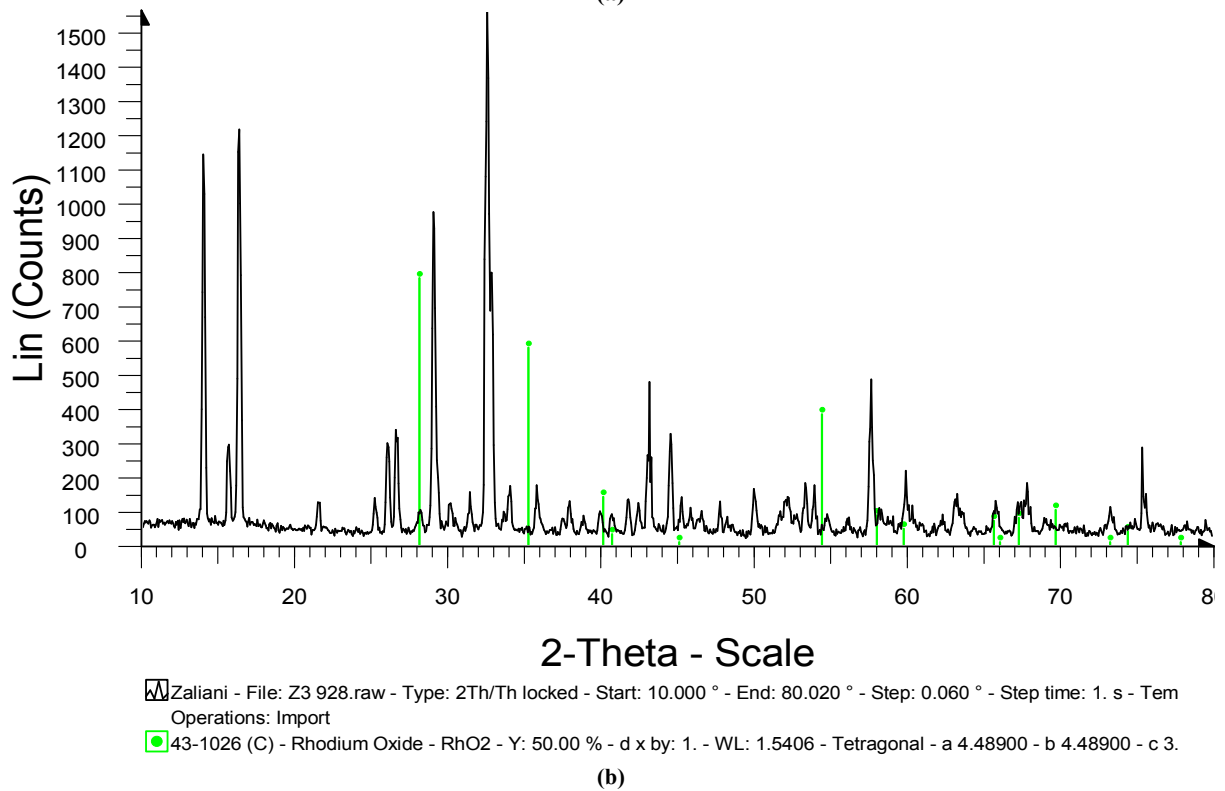
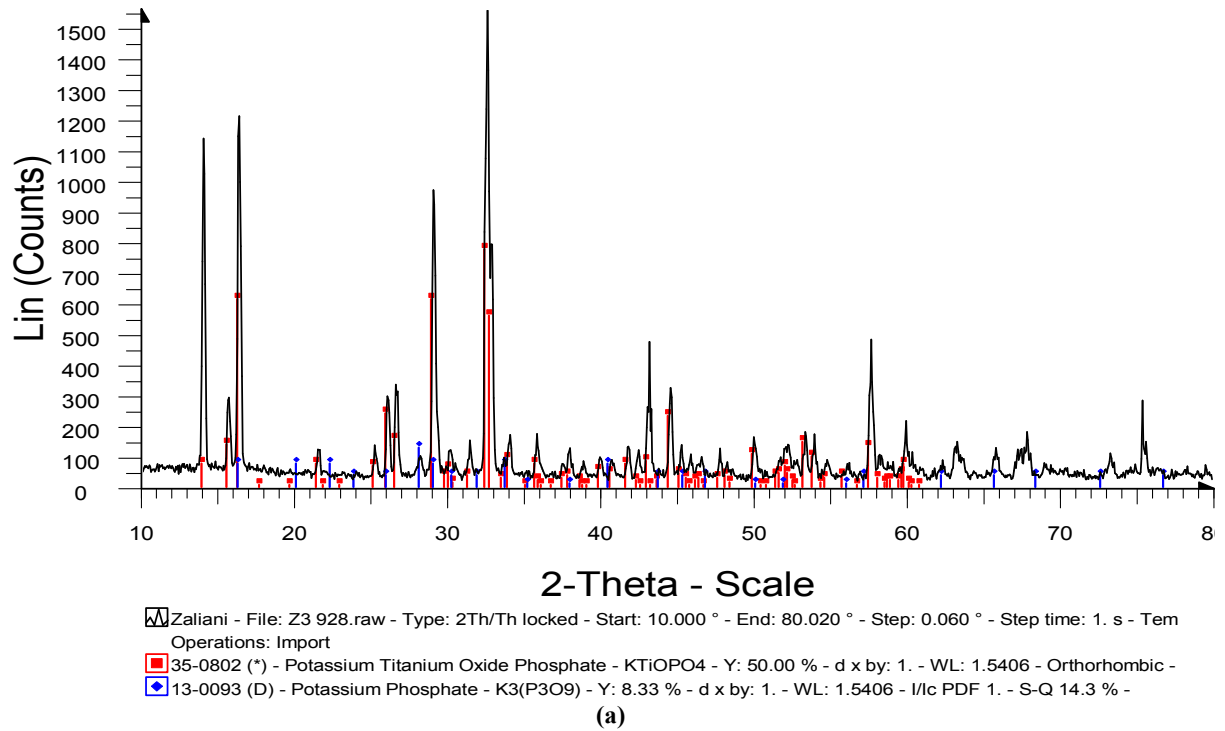


Figure 5. XRD pattern of KTP3 sample: a) to confirm the growth of  $\text{KTiPO}_4$  crystal, b) to detect the existence of  $\text{RhO}_2$  impurity.

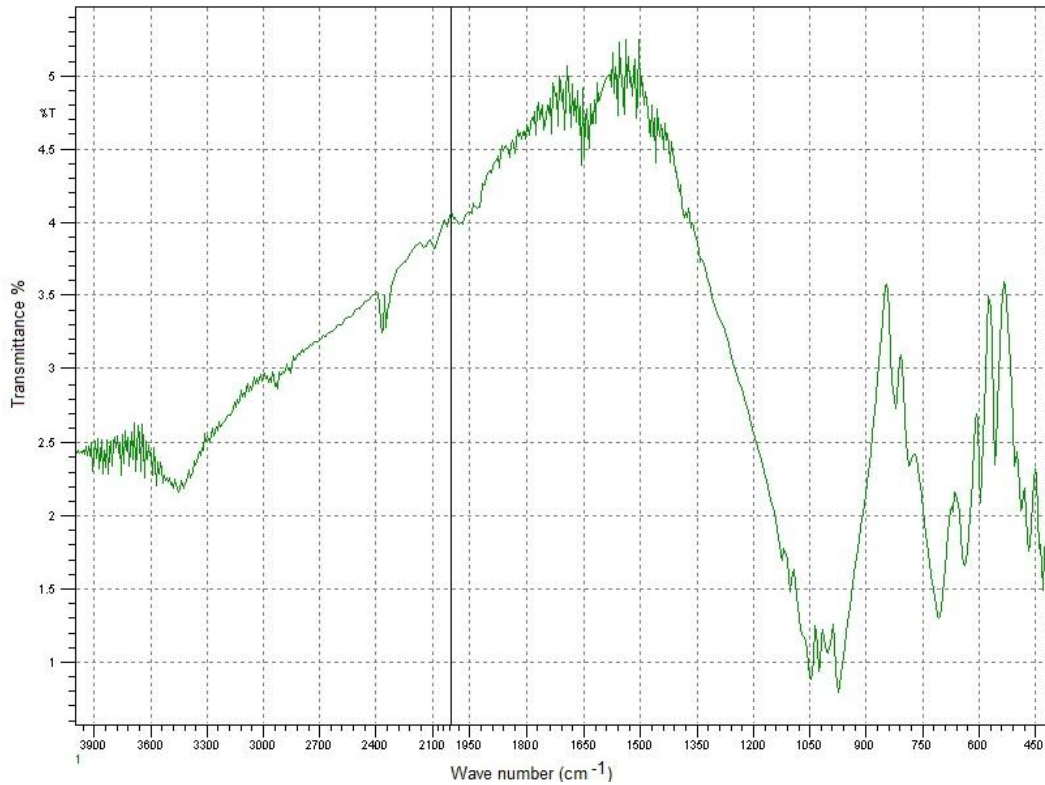


Figure 6. IR spectrum of KTP crystal grown from K<sub>6</sub> flux.

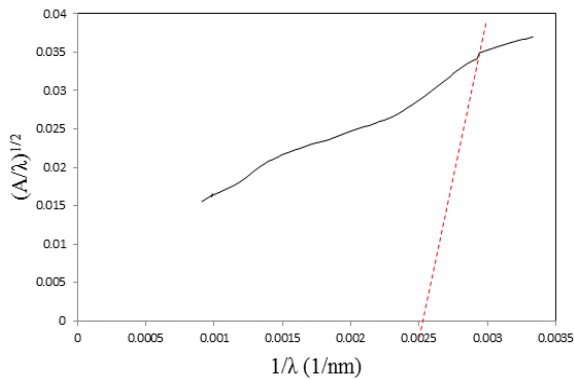


Figure 7. The absorption spectrum of KTP crystals grown from K<sub>6</sub> flux by spontaneous nucleation with cooling rate of 1 °C/h; KTP1.

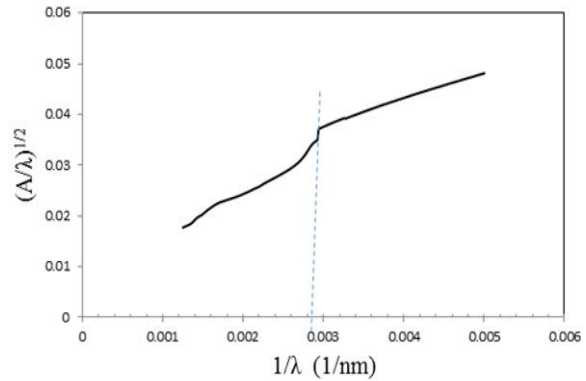


Figure 8. The absorption spectrum of KTP crystals grown from K<sub>6</sub> flux by spontaneous nucleation with cooling rate of 0.8 °C/h; KTP2.

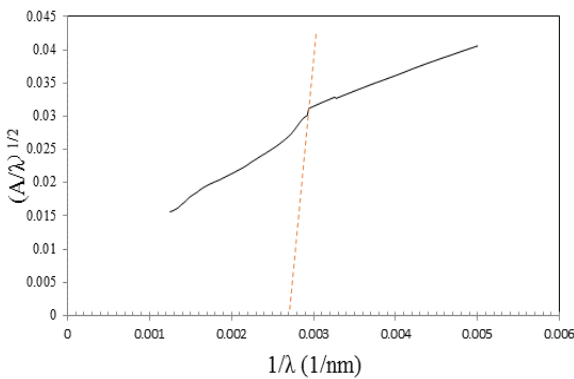


Figure 9. The absorption spectrum of KTP crystals grown from K<sub>6</sub> flux by spontaneous nucleation with cooling rate of 0.4 °C/h; KTP3.

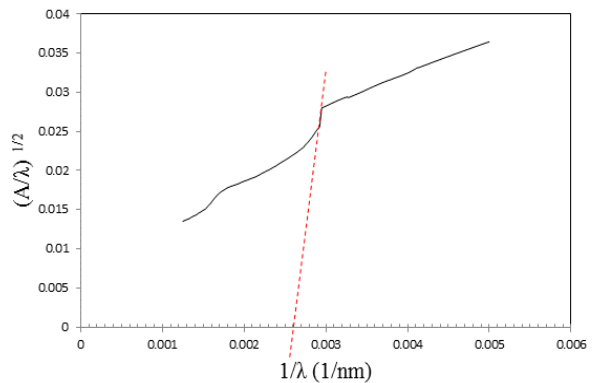


Figure 10. The absorption spectrum of KTP crystals grown from K<sub>6</sub> flux by nucleation on rod with cooling rate of 0.7 °C/h; KTP4.

**Table 3.** Energy band gap of different samples.

samples	Cooling rate (oC/h)	$\lambda_g$ (nm)	$E_{gap}$ (eV)
KTP1	1	342	3.63
KTP2	0.8	355	3.50
KTP3	0.4	377	3.29
KTP4	0.7	360	3.45

crucible result in more reddish colored crystals [3].

The band edge of KTP has been reported to lie between 340 and 360 nm [26-27]. UV transmission cut-off for pure KTP crystals are unlike the colored crystals. From figures 7-10, it is seen that the incorporation of impurity ions such as Rh, shifts the absorption edge of KTP towards UV region by 30 nm. The UV band edge is generally attributed to absorption in the Ti-O subgroup [28-29].

More than 50% transmission was observed in transmission spectra for specimens of thickness exceeding 1mm for crystals grown by nucleation from  $K_6$  flux. Incorporation of impurity ions considerably decreases the overall transmittance of KTP. We saw that incorporation of some impurities from flux and raw materials to crystals is low and did not affect transmission percent and just created some low new peak. For more clarity, it should be mentioned that in KTP1, KTP2 and KTP3 samples which have been grown by the same method (SN), results are (a) upon the XRF analysis, the percent of the principle components increased with decreasing of cooling rate; (b) impurities contents decreased with decreasing of cooling rate; (c) optical transmittance of the mentioned samples increased with decreasing of cooling rate, thus it affects directly on the optical band gap (namely, caused to the decreasing of  $E_g$  as could be predicted). On the other hand, in KTP4 which has been grown by NR method, the percent of the principle components are comparable with what reported for KTP1, 2 and 3 samples; but using this growth method (as improved method), we have the following results: (a) impurities contents decreased; (b) optical transparency and optical transmission increased.

Generation of visible laser wavelengths by SHG of near-IR-wavelength laser beams is a frequent application of KTP. A comparison of transmission at the SHG wavelengths of the 1.064 mm Nd:YAG fundamental laser lines was made for this reason. The SHG wavelength (532 nm) is in the region of reduced transmission [28].

The optical spectra in the 400-700 nm regions are of specific interest in KTP. The absorption in the 500 nm region is probably due to the presence of  $Ti^{+3}$  in different concentrations. The same absorption is induced by electric fields in KTP and was assumed to correspond with the grey track effect [30-34]. Use of KTP as a SHG to convert 1064 nm to 532 nm requires a minimum absorption at 532 nm. This absorption is probably involved in the grey track formation mechanism. The presence of  $Ti^{+3}$  in phosphate glasses has been shown to result in a broad absorption band over the 400-700 nm region [35]. It was suggested that the absorption near 400 nm or 390 nm may be due to either  $Fe^{2+}$  or  $Fe^{4+}$  ions [36-38] that we observed this ions at the XRF data, too. Scripsick et al [39] attributed the 500 nm band to the

gray-track effect to the fact that gray tracks are formed in flux-grown KTP when isolated  $Fe^{3+}$  ions trap holes and  $Ti^{4+}$  ions (with an adjacent oxygen vacancy) trap [39].

The major peaks are at 450, 560 and 725 nm. These absorptions are due to a charge-transfer transition in  $Ti^{+3}$ - $Ti^{+4}$  pairs (450 nm) and the other two to the Jahn-Teller effect which causes a tetragonal distortion in the octahedral coordination polyhedron. It is well known that when two ions occupy adjacent, identical lattice sites in an insulating crystal, transfer of an electron between them does not involve a change in energy. In this case, there would be no optical absorption. However, if the ions are on different sites, an energy difference does exist and optical absorption will be observed. This is probably the case for  $Ti^{+3}$  and  $Ti^{+4}$  ions in KTP, so the presence of  $Ti^{+3}$  in KTP as the source for this absorption [34] is justified. The presence of an impurity such as Pb or Rh could cause a reduction in the oxidation state of  $Ti^{+4}$  to  $Ti^{+3}$  and also increase the concentration of K vacancies. All of these factors could result in an increased susceptibility of KTP to grey track damage [31]. In addition, as presented in figures 5-a and b, XRD outputs confirm the growth of KTP crystal and the presence of small amount of Rh impurity. Figure 5-a was in excellent matching with the 35-0802 standard and the presence of  $RhO_2$  impurity was checked, which was in relatively good matching with the standard code of 43-1026; XRD outputs show an orthorhombic structure with the lattice parameters of  $a=12.814 \text{ \AA}$ ,  $b=10.816 \text{ \AA}$  and  $c=6.404 \text{ \AA}$ . On the other hand, to more confirm the growth of KTP crystals, IR study was performed and the spectrum of the sample grown from  $K_6$  flux is shown in figure 6; main absorption bands are located at about 409, 432, 468, 489, 505, 557, 596, 640, 708, 787, 821, 831, 976, 1004, 1026, 1049, 1101, 1124, 1650, 2380 and  $3500 \text{ cm}^{-1}$ . For example, vibration modes especially around 1049, 1101 and  $976 \text{ cm}^{-1}$  are related to  $PO_4$  tetrahedral units and the band of 1124 justify the presence of P-O bonds. Also, absorption peaks of 409, 596 and 708 are in consistency with  $TiO_6$  octahedra [17]. Bands of 1650, 2380 and  $3500 \text{ cm}^{-1}$  are related to  $H_2O$  due to small ambient and sample humidity. In brief, IR output confirms and justifies again the growth of KTP crystal from flux.

## 6. Conclusions

Transmission measurements in KTP were performed. XRF studies confirmed the incorporation of impurity content in the crystals grown from kind of fluxes. The incorporation of impurity ions into the grown crystal is presumed to shift the optical absorption edge towards the UV region and increases the optical absorption. Structural elucidation was carried out employing XRD and IR analysis, confirming the growth of KTP crystals.

**Acknowledgement**

The authors gratefully acknowledges Mrs Elaheh

Gharibshahian for her technical support.

**References**

1. F C Zumsteg, J D Bierlein, and T E Gier, *J. Appl. Phys.* **47** (1976) 4980.
2. M Jaber, A H Farahbod, and H Rahimpur Soleimani, *Iranian Journal of Physics Research*, **13**, 1, (2013) 35.
3. I Bhaumik, S Ganesamoorthy, R Bhatt, A K Karnal, R Sundar, and V K Wadhawan, *Cryst. Res. Technol.* **41** (2006) 1180.
4. J C Jacco, G M Loiacono, M Jaso, G Mizell, and B Greenberg, *J. Cryst. Growth*. **70** (1984) 484.
5. C V Kannan, S Ganesamoorthy, S Kumaragurubaran, C Subramanian, R Sundar, and P Ramasamy, *Cryst. Res. Technol.* **37** (2002) 1049.
6. P F Bordui and S Motakef, *J. Cryst. Growth*. **96** (1989) 405.
7. T Sasaki, A Miyamoto, A Yokotani, and S Nakai, *J. Crystal. Growth*. **128** (1993) 950.
8. S Ganesamoorthy, F Josephkumar, S Balakumar, C Subramanian, and P Ramasamy, *Mat. Sci. Eng. B* **60** (1999) 88.
9. G M Loiacono, T F McGee, and G Kostecky, *J. Cryst. Growth*. **104** (1990) 389.
10. I Bhaumik, S Ganesamoorthy, R Bhatt, R Sundar, A K Karnal, and V K Wadhawan, *J. Cryst. Growth*. **243** (2002) 522.
11. L P Shi, J Chrosch, J W Wang, and Y G Liu, *Cryst. Res. Technol.* **27** (1992) 76.
12. S Haussuhl, S Luping, W Banlia, W Jiyang, J Liebertz, A Wostrack, and C Fink, *Cryst. Res. Technol.* **29** (1994) 583.
13. R J Bolt, H De Haas, M T Sebastian, and H Klapper, *J. Crystal Growth*. **110** (1991) 587.
14. P J Halfpenny, L O Neill, J N Sherwood, G S Simpson, A Yokotani, A Miyamoto, T Sasaki, and S Nakai, *J. Crystal. Growth*. **113** (1991) 722.
15. A Yokotani, A Miyamoto, T Sasaki, and S Nakai, *J. Crystal Growth*. **110** (1991) 963.
16. T Sasaki, A Miyamoto, A Yokotani, and S Nakai, *J. Cryst. Growth*. **129** (1993) 950.
17. E Gharibshahian, M J Tafreshi, and M Fazli, *Indian J. Pure Appl. Phys.* **47** (2009) 356.
18. E Gharibshahian and M J Tafreshi, *Cryst. Res. Technol.* **50**, 8 (2015) 603.
19. J R Ghandhi, M Rathnakumari, P Muralimanohar, P Sureshkumar, and G Bhagavannarayana, *J. Appl. Crystallography* **47** (2014) 931.
20. J R Ghandhi, B Vijayalakshmi, M Rathnakumari, and P Sureshkumar, *Journal of Minerals & Materials Characterization & Engineering* **10**, 8 (2011) 683.
21. J R Ghandhi, M Rathnakumari, K Ramamurthi, R R Babu, D Sastikumar, and P Sureshkumar, *Optik* **125** (2014) 6462.
22. A Miyamoto, Y Mori, and T Sasaki, *Appl. Phys. Lett.* **69** (1996) 1032.
23. CV Kannan, S Ganesamoorthy, H Kimura, and A Miyazaki, *J. Crystal. Growth* **279** (2005) 403.
24. D Souri and K Shomalian, *J. Non-Cryst. Solids* **355** (2009) 1597.
25. K De, "A Textbook of Inorganic Chemistry", Wiley Eastern Limited, New Delhi, 7<sup>th</sup> ed. (1992).
26. D Bierlein and H Vanherzeele, *J. Opt. Soc. Am. B* **6** (1989) 622.
27. V V Lemesko, V V Obukhovskiy, V Stoyanov, N I Pavlova, A I Pisanskiy, and P A Korotkov, *Ukrain. Fiz. Zh.* **31** (1986) 1746.
28. G Hansson, H Karlsson, S Wang, and F Laurell, *Appl. Optics*. **39** (2000) 5058.
29. J C Jacco and G M Loiacono, *Appl. Phys. Lett.* **58** (1990) 560.
30. R Blachman, P F Bordui, and M M Fejer, *Appl. Phys. Lett.* **64** (1994) 1318.
31. G M Loiacono, D N Loiacono, T McGee, and M Babb, *J. Appl. Phys.* **72** (1992) 2705.
32. M G J Roelofs, *Appl. Phys.* **65** (1989) 4976.
33. K Terashima, M Takena, and M Kawachi, *Jpn. J. Appl. Phys.* **30** (1991) 497.
34. N B Angert, V M Garmash, N I Pavlova, and A V Tarasov, *Sov. J. Quantum Electron.* **21** (1991) 426.
35. L E Bausa, J G Sole, A Duran, and J M F Navarro, *J. Non-Cryst. Solids* **127** (1991) 267.
36. M J Martin, D Bravo, R Sole, F Diaz, F J Lopez, and C Zaldo, *J. Appl. Phys.* **76** (1994) 7510.
37. M J Martin, C Zaldo, F Diaz, R Sole, D Bravo, and F J Lopez, *Radiat. Eff. Defects Solids* **136** (1995) 243.
38. L E Halliburton and M P Scripsick, *Proc. SPIE* **235** (1995) 2379.
39. M P Scripsick, D N Loiacono, J Rottenberg, S H Goellner, L E Halliburton, and F K Hopkins, *Appl. Phys. Lett.* **66** (1995) 3428.